Author's Accepted Manuscript

One-pot Solution Coating of High Quality LiF Layer to Stabilize Li Metal Anode

Jialiang Lang, Yuanzheng Long, Jiale Qu, Xinyi Luo, Hehe Wei, Kai Huang, Haitian Zhang, Longhao Qi, Qianfan Zhang, Zhengcao Li, Hui Wu

energy storage materials

Cite this article as: Jialiang Lang, Yuanzheng Long, Jiale Qu, Xinyi Luo, Hehe Wei, Kai Huang, Haitian Zhang, Longhao Qi, Qianfan Zhang, Zhengcao Li and Hui Wu, One-pot Solution Coating of High Quality LiF Layer to Stabilize Li Metal Anode, *Energy Storage Materials,* https://doi.org/10.1016/j.ensm.2018.04.024

One-pot Solution Coating of High Quality LiF Layer to Stabilize Li Metal Anode

Jialiang Lang[a,b,1], Yuanzheng Long[a,1], Jiale Qu[c,1], Xinyi Luo[b], Hehe Wei[a], Kai Huang[a], Haitian Zhang[a], Longhao Qi[a], Qianfan Zhang[*,c], Zhengcao Li[*,b], Hui Wu[*,a]

[a] State Key Lab of New Ceramic and Fine Processing, School of Materials Science and Engineering, Tsinghua University, Beijing 100084, China

[b] Key Laboratory of Advanced Materials, School of Materials Science and Engineering, Tsinghua University, Beijing 100084, China

[c] School of Materials Science and Engineering, Beihang University, Beijing 100191, China

huiwu@tsinghua.edu.cn (H. Wu),
zcli@tsinghua.edu.cn (Z. Li),
qianfan@buaa.edu.cn (Q. Zhang)
*Corresponding author: Hui Wu
*Corresponding author: Zhengcao Li
*Corresponding author: Qianfan Zhang

Abstract

The high reactivity of Li metal anodes towards liquid electrolytes leads to an unstable and accumulated solid electrolyte interphase (SEI) film, which results in dendrite growth and low Coulombic efficiency (CE). Lithium fluoride (LiF) coating is considered as a reliable and dense SEI film to protect the reactive anode, however, the chemistry to form uniform, conformal and high quality LiF protection layer on Lithium metals remains as a major challenge. Here we develop a simple solution method to obtain LiF coating on Li metal anodes. We have discoverd a chemical method to fabricate LiF coating via the in-situ reaction between metallic Li and polyvinylidene fluoride (PVDF)-dimethyl formamide (DMF) solution. Owing to the chemically and mechanically stable artificial SEI film, the LiF-coated Li anode

delivers a better cycling performance than bare Li anode under various current densities in symmetrical cells. Stable cycling over 300 plating/striping cycles was achieved with LiF-coated Li electrodes under a high current density of 3 mA cm^{-2}. The LiF coating also effectively suppresses dendrite formation and reduces side reactions between the metallic Li and the carbonate-based electrolyte. Therefore, this simple and low-cost method may benefit the future applications of the next generation Li metal batteries.

Keywords: Lithium metal battery, lithium metal anode, LiF coating, solid electrolyte interphase, stable cycling

1. Introduction

Research on rechargeable batteries has made great progress in the past few decades, especially the research of the lithium ion batteries (LIBs)[1-4]. However, the energy density of commercial LIBs has very limited room for improvement, which makes it difficult for LIBs to meet the increasing demands of electric vehicles and portable electronics [5-6]. Li metal batteries have potentials to realize a higher energy density owing to their high theoretical capacity (3860 mAh g^{-1}) and the low electrochemical potential (−3.04 V vs the standard hydrogen electrode) of Li metal anodes. Nevertheless, the high reactivity of metallic Li and the huge volume change during Li plating/striping cycles result in an unstable SEI film when using liquid organic electrolytes [7]. As a result, Li metal batteries suffer from persistent side reactions between anodes and electrolytes, Li dendrite growth, low CE, and severe consumption of the electrolyte [8]. Therefore, to improve the cycling performance of

Li metal anodes and avoid safety issues caused by dendrite growth, a chemically and mechanically stable SEI film is necessary [9-14].

Great efforts have been made to solve the interfacial issues and construct a robust SEI film [15-20]. Engineering the liquid electrolytes is a straightforward method to enhance the stability of the SEI film. By adding additives, using high concentrated electrolytes and employing new type liquid electrolytes, the interfacial stability can be significantly improved [21-26]. A functional coating on Li metal anodes can also contribute to the enhancement of the interfacial stability, especially an artificial SEI layer. Guo's group demonstrated that the Li_3PO_4 SEI layer by in situ reaction of polyphosphoric acid with Li metal could suppress dendrite growth and restrain side reactions between Li metal anodes and liquid electrolytes [27]. LiF is also an ideal SEI film owing to its high chemical stability, low solubility in carbonate based electrolytes and high shear modulus [28, 29]. Recently, Cui's group demonstrated that the uniform LiF coating on Li metal anode could effectively prevent the corrosion reaction of carbonate electrolytes and enhance the performance of Li anodes [30].

Herein, we report a mild and scalable method for fabricating LiF-coated Li anodes at an acceptable cost. As shown in Fig. 1a, a common separator, soaked in the PVDF-DMF solution previously was pasted onto a polished Li foil for five seconds before being removed. After the volatilization of the small residual solution, a Li anode with an artificial LiF SEI layer was obtained. We reason that the LiF coating on Li anode can effectively minimize the side reaction with electrolytes and hinder the dendrite formation (Fig. 1b). By contrast, the pristine SEI film of bare Li anode is

vulnerable to defects due to the infinite volume change during plating/striping cycles, which leads to dendrite formation and growth (Fig. 1c). LiF-coated anodes deliver significant enhanced cyclic stability compared to bare Li anodes in both symmetrical cells and full cells with $LiCoO_2$ as cathodes in a carbonate electrolyte.

2. Experimental Section

2.1 Formation of LiF on lithium metal

To illustrate the reaction mechanism between metallic Li and PVDF-DMF solution, we directly dropped the PVDF-DMF solution on the Li foil (Video S1). After about 40 seconds, the solution started to turn blue and then became darker, while, as shown in Video S2, there was no obvious change when dropping pure DMF solution on the Li foil. The final product is black and the microstructure of the black layer is shown in Fig. 2a. Compared with the uniform morphology of bare Li (Fig. S1), the black product is filled with cracks. The Fourier transform infrared (FTIR) spectrum of the black film on Li shows the peak at 1650 cm^{-1}, which is associated mainly with the formation of C=C double bonds (Fig. 2b)[31]. Instead, the FTIR spectrum of the sample fabricated by dropping PVDF-DMF solution on copper foil shows no peak around 1650 cm^{-2}, which indicates that there is nearly no existence of C=C double bonds in the pristine PVDF powder (Fig. 2b). The X-ray photoelectron spectroscopy (XPS) results shown in Fig. 2c and Fig. S2 indicate the existence of LiF in the black film. The gas chromatography (GC, Fig. 2d) results indicate the generation of H_2 during the reaction between metallic Li and PVDF-DMF solution, while there is nearly no release of H_2 when dipping Li foil into pure DMF. Based on the FTIR, GC

and the XPS results, we speculate that the dehydrofluorination process of PVDF occurs under the synergistic effect of DMF and metallic Li, which then leads to the formation of LiF, C=C double bonds and H_2. To verify the synergistic effect of DMF, ^{1}H nuclear magnetic resonance (NMR) measurement on pure DMF and the PVDF-DMF solution was conducted. As shown in Fig. S3, both the two resonances of methyl protons and the resonance of HCO proton for PVDF-DMF solution shift to downfield, indicating the decrease in the electron density of amide group due to the H-bonding interactions between amide group in DMF molecules and H atom in PVDF. The electron-enriched N and O atoms of DMF donate pairs of electrons and facilitate the dehydrofluorination of PVDF [28]. We also used other solvents, including dimethylacetamide (DMAc), N-methyl pyrrolidone (NMP), dimethyl carbonate (DMC) and methoxymethane (DME), to prepare PVDF solutions instead of DMF. As shown in Fig. S4, there was no obvious change when dropping other PVDF solutions on the Li foil, indicating that the DMF plays an important role during the reaction between PVDF and metallic Li.

We speculate that DMF does not take part in the reaction directly. To verify it, a Li foil was dipped into the PVDF-DMF solution for 2 min, and then removed. The solution appeared dark blue, which was possibly caused by the conjugate effect of C=C double bonds and C-C single bond [32]. The FTIR spectra of the solution before and after reaction with Li are shown in Fig. S5. No remarkable changes of the peaks corresponding to DMF were observed. The ^{1}H NMR spectra (Fig. S6) also indicate no change of DMF. The two peaks at ~2.8 ppm are for the methyl protons,
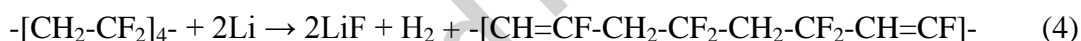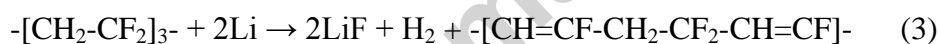
and the peak at ~7.94 ppm for the CHO proton.

2.2 Computation.

To evaluate the thermodynamic stability of reactions between Li metal and PVDF, we computed the formation energy corresponding to the reaction, which can be expressed as

$$E_F = [\Sigma E \ (reactant) - \Sigma E \ (resultant)]/x \qquad (1)$$

ΣE (resultant) represents the total energy of resultants; *ΣE (reactant)* represents that of the reactant, while x is the number of Li ions involved in reaction. According to this definition, a positive (negative) E_F means that the reaction is an exothermic (endothermic) process. To simulate different possible polymer resultants in a real reaction (Fig. 2e), we considered three different kinds of resultants: poly 1,3-double-fluorinated-diene, poly-1, 3, 3, 5-four-fluorinated-diene and poly-1, 3, 3, 5, 5, 7-six-fluoroded-diene. We compared the E_F in different reactions, the reaction equations can be expressed as (2)-(4) respectively:

$$-[CH_2-CF_2]_2- + 2Li \rightarrow 2LiF + H_2 + -[CH=CF-CH=CF]- \qquad (2)$$

$$-[CH_2-CF_2]_3- + 2Li \rightarrow 2LiF + H_2 + -[CH=CF-CH_2-CF_2-CH=CF]- \qquad (3)$$

$$-[CH_2-CF_2]_4- + 2Li \rightarrow 2LiF + H_2 + -[CH=CF-CH_2-CF_2-CH_2-CF_2-CH=CF]- \qquad (4)$$

The E_F corresponding to three different resultants are 3.75 eV, 3.70 eV and 3.62 eV, respectively, indicating that the reaction is energetically favorable and has a high probability to happen. The E_F magnitudes for different resultant chains are almost the same. Therefore, we can also speculate that the real situation of resultant should be a mix of different chain structures.

2.3 Synthesis.

To fabricate LiF-coated Li anodes, a common separator previously soaked in the PVDF-DMF solution was placed on a polished Li foil for five seconds and then taken away. The morphology of the LiF-coatied Li is shown in Fig. 3a. The LiF film is uniform and dense with a thickness of ~ 300 nm (Fig. 3b), which is characterized by

focused ion beam-scanning electron microscopy (FIB-SEM). The XPS (Fig. S7) reveals the major component of the Li coating is LiF.

2.4 Electrochemical Measurements.

To investigate the electrochemical performance of LiF-coated Li anodes, symmetrical cells were assembled using a carbonate-based electrolyte. Cyclic voltammetry (CV) measurements were conducted to evaluate the Li plating and stripping behavior. A Cu disk was used as the working electrode and the as-prepared LiF-coated Li as the reference and counter electrode. As shown in Fig. S8, the current intensity of both plating and striping processes during the first two cycles exhibits only minimal change possibly due to the stable interface between the LiF-coated Li and the electrolyte. The artificial SEI is expected to function as a passivation layer to minimize the side reactions between metallic Li and liquid electrolyte. As a result, the symmetrical cells with LiF-coated Li anodes outperformed the bare Li symmetrical cells at various current densities (Fig. 4 a,b,c). The overpotential of the bare Li cell started to increase gradually after 180 cycles at the current density of 3 mA cm^{-2}, while the overpotential of the LiF-coated Li cell was stable with nearly no increase (Fig. 4b). Similar things happened when using a higher current density of 5 mA cm^{-2}. The typical voltage profiles of one plating/striping cycle under different current densities are shown in Fig. S9, revealing the overpotential of the LiF-coated Li cells is much lower than that of the bare Li cell. For the bare Li cells, the increasing overpotential is caused by both the accumulated 'dead' SEI film and the sustaining consumption of electrolyte. The LiF-coated Li cell also delivers a better performance

with a high areal capacity of 3 mAh cm^{-2} at a high current density of 3 mA cm^{-2} than the bare Li cell (Fig. S10). Furthermore, the Li|LiCoO$_2$ batteries with an areal capacity of 1 mAh cm^{-2} were tested to demonstrate the high performance of LiF-coated Li anodes in full batteries (Fig. 4d). The full battery with a LiF-coated Li anode delivered a capacity retention of 85.7% after 200 cycles. In contrast, the capacity of the bare Li full cell decayed significantly after 200 cycles.

To further study the stability of LiF-coated Li anodes, the symmetrical cells with LiF-coated Li were disassembled after 100 cycles at the current density of 1 mA cm^{-2}. The morphology of the LiF-coated Li electrode was characterized by SEM. As shown in Fig. 5a, b, the surface of the LiF-coated Li electrode generally remains flat with some cracks, but no obvious dendrites, which indicates the LiF coating is mechanically and electrochemically stable during Li plating/striping cycles. In contrast, the bare Li electrode possesses a rough surface filled with cracks, which are obvious even at a low magnification (Fig. 5c). The SEM image of the bare Li anode with higher magnification shows that the bare Li exhibits a porous structure with massive dendrites (Fig. 5d). With LiF coating, the Li metal underneath generally keeps a dense and stable structure, indicating that the artificial SEI layer effectively suppresses the corrosion reaction caused by the carbonate electrolyte [33, 34]. Electrochemical impedance spectroscopy (EIS) was conducted on the symmetric cells before cycling and after 100 cycles at 1 mA cm^{-2} (Fig. S11 and Fig. S12). The lower impedance of the LiF-coated Li cell at both stages might be due to the chemical stability of the LiF coating. The XPS analysis of the Li electrodes after 100 cycles

indicates that the SEI film of LiF-coated Li electrodes possesses a higher component of LiF than that of bare Li electrode (Fig. S13). Besides the better electrochemical performance, the LiF-coated Li also delivers higher stability in air than bare Li, which might benefit processing in an industrial setting (Fig. S14).

3. Conclusion

In conclusion, we report a simple and mild method to fabricate LiF-coated Li electrodes with low cost. Via an in situ reaction between Li metal and PVDF-DMF solution, a uniform and stable LiF coating is formed on the surface of Li metal. The reaction mechanism is verified both experimentally and theoretically. The LiF coating not only effectively minimizes the side reactions between metallic Li and liquid electrolytes, but also suppresses dendrite growth. Therefore, this artificial SEI layer enhances the cycling stability of Li metal electrodes both in symmetrical cells and in full cells. Moreover, this moderate and scalable method may also apply to the protection of sodium electrodes and other active metal electrodes.

Associated A. Supporting Information

Supplementary data associated with this article can be found in the online version at

References

[1] K. Jiang, X. Wu, Y. Yin, J. Lee, J. Kim, Y. Guo, Superior Hybrid Cathode Material Containing Lithium-Excess Layered Material and Graphene for Lithium-Ion Batteries, ACS Appl. Mater. Interfaces 4 (2012) 4858-4863.

[2] J. B. Goodenough, K. Park, The Li-Ion Rechargeable Battery: A Perspective, J. Am. Chem. Soc. 135 (2013) 1167-1176.

[3] K. Qian, L. Tang, M. Wagemaker, Y. He, D. Liu, H. Li, R. Shi, B. Li, F. Kang, A Facile Surface Reconstruction Mechanism toward Better Electrochemical Performance of $Li_4Ti_5O_{12}$ in Lithium‐Ion Battery, Adv. Sci. 4 (2017) 1700205.

[4] L. Tang, Y. He, C. Wang, S. Wang, M. Wagemaker, B. Li, Q. Yang, F. Kang, High-Density Microporous $Li_4Ti_5O_{12}$ Microbars with Superior Rate Performance for Lithium-Ion Batteries, Adv. Sci. 4 (2017) 1600311

[5] J. –M. Tarascon, M. Armand, Issues and challenges facing rechargeable lithium batteries, Nature 414 (2001) 359-367.

[6] J. B. Goodenough, Y. Kim, Challenges for Rechargeable Li Batteries, Chem. Mater. 22 (2010) 587-603.

[7] X. Cheng, R. Zhang, C. Zhao, Q. Zhang, Toward Safe Lithium Metal Anode in Rechargeable Batteries: A Review, Chem. Rev. 117 (2017) 10403-10473.

[8] D. Lin, Y. Liu, Y. Cui, Reviving the lithium metal anode for high-energy batteries, Nat. Nanotechnol. 12 (2017) 194–206.

[9] Y. Gao, R. Li, Y. Li, J. Song, S. Chen, Q. Huan, T.E. Mallouk, D.Wang, Generating System-Level Responses from a Network of Simple Synthetic Replicators, J. Am. Chem. Soc. 139 (2017) 17565-17573.

[10] J. Lang, L. Qi, Y. Luo, H. Wu, High performance lithium metal anode: Progress and prospects, Energy Storage Mater. 7 (2017) 115-129.

[11] C. Jin, O. Sheng, J. Luo, H. Yuan, C. Fang, W. Zhang, H. Huang, Y. Gan, Y. Xia, C. Liang, J. Zhang, X. Tao, 3D lithium metal embedded within lithiophilic porous matrix for stable lithium metal batteries, Nano Energy 37 (2017) 177-186.

[12] J. Lang, Y. Jin, X. Luo, Z. Liu, J. Song, Y. Long, L. Qi, M. Fang, Z. Li, H. Wu, Surface graphited carbon scaffold enables simple and scalable fabrication of 3D composite lithium metal anode, J. Mater. Chem. A 5 (2017) 19168-19174.

[13] L. Liu. Y. Yin, J. Li, N. Li, X. Zeng, H. Ye, Y. Guo, L. Wan, Free-Standing Hollow Carbon Fibers as High-Capacity Containers for Stable Lithium Metal Anodes, Joule 1 (2017) 563-575.

[14] C. Yang, K. Fu, Y. Zhang, E. Hitz, L. Hu, Protected Lithium-Metal Anodes in Batteries: From Liquid to Solid, Adv. Mater. 29 (2017) 1701169.

[15] X. Cheng, H. Peng, J. Huang, R. Zhang, C. Zhao, Q. Zhang, Dual-Phase Lithium Metal Anode Containing a Polysulfide-Induced Solid Electrolyte Interphase and Nanostructured Graphene Framework for Lithium–Sulfur Batteries, ACS Nano 9 (2015) 6373-6382.

[16] X. Liang, Q. Pang, I. Kochetkov, M. Sempere, H. Huang, X. Sun, L. Nazar, A facile surface chemistry route to a stabilized lithium metal anode, Nature Energy 2 (2017) 17119.

[17] X. Zhang, X. Cheng, X. Chen, C. Yan, Q. Zhang, Fluoroethylene carbonate additives to render uniform Li deposits in lithium metal batteries, Adv. Funct. Mater. 27 (2017) 1605989.

[18] S. Huang, L. Tang, H. S. Najafabadi, S. Chen, Z. Ren, A highly flexible semi-tubular carbon film for stable lithium metal anodes in high-performance batteries, Nano Energy 38 (2017) 504-509.

[19] S. Wang, Y. Yin, T. Zuo, W. Dong, J. Li, J. Shi, C. Zhang, N. Li, C. Li, Y. Guo, Stable Li Metal Anodes via Regulating Lithium Plating/Stripping in Vertically Aligned Microchannels, Adv. Mater. 29 (2017) 1703729.

[20] F. Ding, W. Xu, G. Graff, J. Zhang, M. Sushko, X. Chen, Y. Shao, M.H. Engelhard, Z. Nie, J. Xiao, X. Liu, P.V. Sushko, J. Liu, J.G. Zhang, Dendrite-Free Lithium Deposition via Self-Healing Electrostatic Shield Mechanism, J. Am. Chem. Soc. 135 (2013) 4450-4456.

[21] L. Suo, Y. Hu, H. Li, M. Armand, L. Chen, A new class of Solvent-in-Salt electrolyte for high-energy rechargeable metallic lithium batteries, Nat. Commun. 4 (2013) 1481.

[22] M. D. Tikekar, S. Choudhury, Z. Tu, L. Archer, Design principles for electrolytes and interfaces for stable lithium-metal batteries, Nat. Energy 1 (2016) 16114.

[23] X. Cheng, R. Zhang, C. Zhao, F. Wei, J. Zhang, Q. Zhang, A review of solid electrolyte interphases on lithium metal anode, Adv. Sci. 3 (2016) 1500213.

[24] S. Choudhury, A. Agrawal, S. Wei, E. Jeng, L. Archer, Hybrid Hairy Nanoparticle Electrolytes Stabilizing Lithium Metal Batteries, Chem. Mater. 28 (2016) 2147-2157.

[25] X. Shen, H. Liu, X. Cheng, C. Yan, J. Huang, Beyond lithium ion batteries: Higher energy density battery systems based on lithium metal anodes, Energy Storage Mater. 12 (2018) 161-175.

[26] F. Shen, F. Zhang, Y. Zheng, Z. Fan, Z. Li, Z. Sun, Y. Xuan, B. Zhao, Z. Lin, X. Gui, X. Han, Y. Cheng, C. Niu, Direct growth of 3D host on Cu foil for stable lithium metal anode, Energy Storage Mater. 13 (2018) 323-328.

[27] N. Li, Y. Yin, C. Yang, Y. Guo, An artificial solid electrolyte interphase layer for stable lithium metal anodes, Adv. Mater. 28 (2016) 1853.

[28] X. Zhang, T. Liu, S. Zhang, X. Huang, B. Xu, Y. Lin, B. Xu, L. Li, C. Nan, Y. Shen, Synergistic Coupling between $Li_{6.75}La_3Zr_{1.75}Ta_{0.25}O_{12}$ and Poly(vinylidene fluoride) Induces High Ionic Conductivity, Mechanical Strength, and Thermal Stability of Solid Composite Electrolytes, J. Am. Chem. Soc. 139 (2017) 13779-13785.

[29] Y. Gao, Y. Zhao, Y. Li, Q. Huang, T. Mallouk, D. Wang, Interfacial Chemistry Regulation via a Skin-Grafting Strategy Enables High-Performance Lithium-Metal Batteries, J. Am. Chem. Soc. 139 (2017) 15288-15291.

[30] J. Zhao, L. Liao, F. Shi, T. Lei, G. Chen, A. Pei, J. Sun, K. Yan, G. Zhou, J. Xie, C. Liu, Y. Li, Z. Liang, Z. Bao, Y. Cui, Surface Fluorination of Reactive Battery Anode Materials for Enhanced Stability, J. Am. Chem. Soc. 139 (2017) 11550-11558.

[31] X. Zhang, X. Chen, R. Xu, X. Cheng, H. Peng, R. Zhang, J. Huang, Q. Zhang, Columnar Lithium Metal Anodes, Angew. Chem. Int. Ed. 56 (2017) 14207-14211.

[32] A. Bottino, G. Capannelli, O. Monticelli, P. Piaggio, Poly(vinylidene fluoride) with improved functionalization for membrane production, J. Membrane Science 166 (2000) 23-29.

[33] A. Pei, G. Zheng, F. Shi, Y. Li, Y. Cui, Nanoscale Nucleation and Growth of Electrodeposited Lithium Metal, Nano Lett. 17 (2017) 1132-1139.

[34] Y. Li, J. Jiao, J. Bi, X. Wang, Z. Wang, L. Chen, Controlled deposition of Li metal, Nano Energy 32 (2017) 241-246.
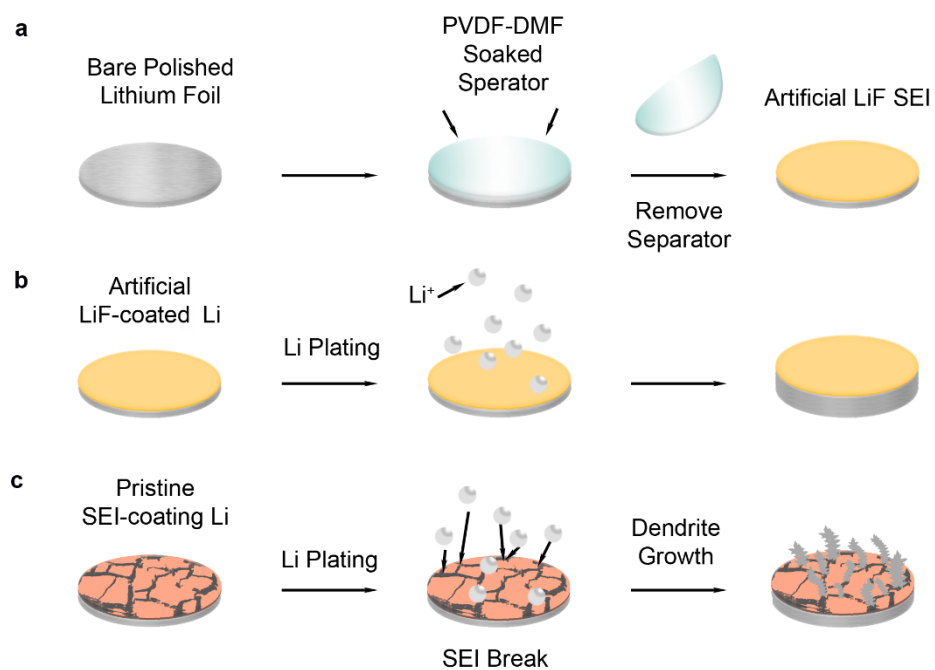
Fig. 1. (a) Illustration of the process for fabricating LiF-coated Li. (b) LiF-coated Li electrodes and (c) bare Li electrodes during SEI formation and cycling.
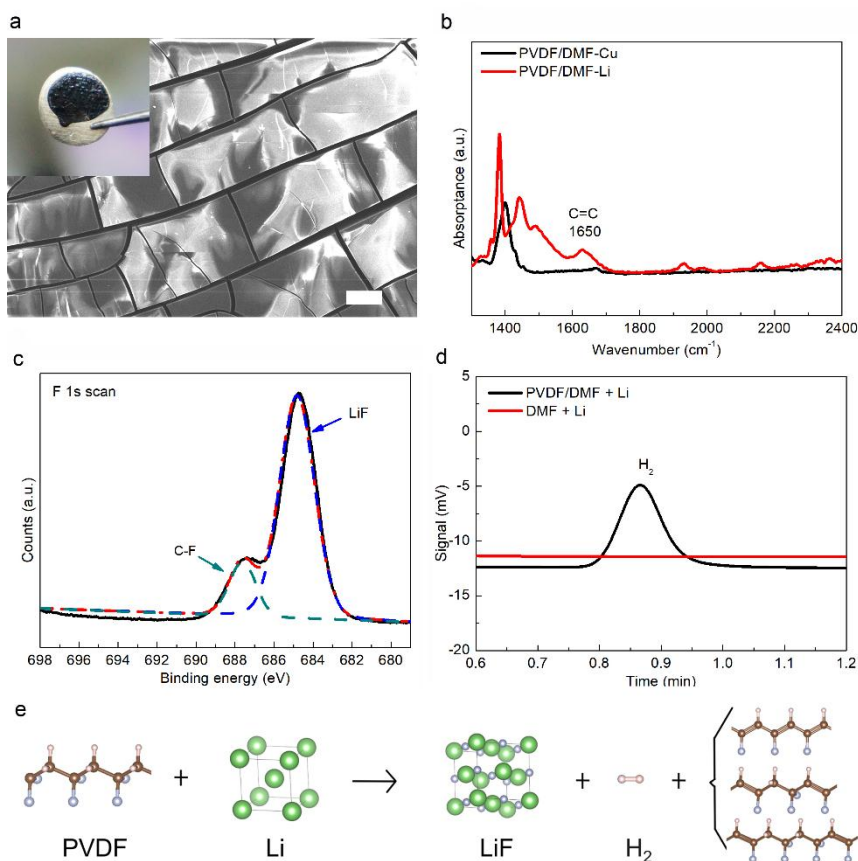
Fig. 2. Reaction mechanism of Li metal and PVDF-DMF solution. (a) SEM image of the black layer on the Li metal produced by the reaction between Li metal and PVDF-DMF solution. The inset is the photograph of the reaction product. Scale bar, 100 μm. (b) FTIR spectra of PVDF film on the copper foil and the black layer on the Li metal. The PVDF film was fabricated by dropping PVDF-DMF solution on the copper foil and then drying it in the ambient conditions. (c) XPS spectrum of the black layer on the Li metal. (d) GC indicating the generation of H_2 during the reaction between Li metal and PVDF-DMF solution. (e) The schematic diagram of the reaction.
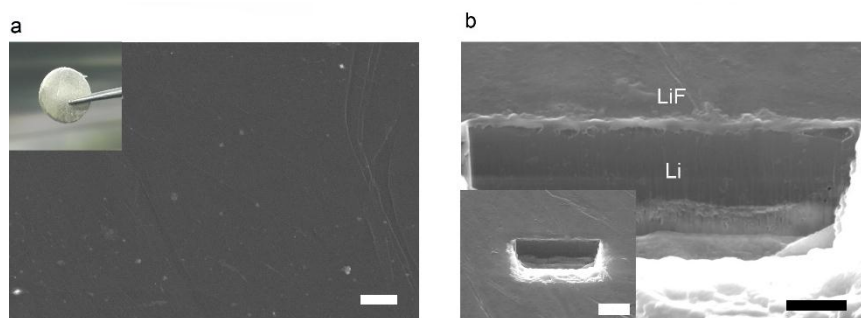
Fig. 3. (a) SEM image of LiF-coated Li. The inset is the photography of LiF-coated Li metal. (b) Cross-sectional FIB-SEM image of LiF-coated Li. The inset is the image with a lower magnification. Scale bar, 10 μm (a), 2 μm (b) and 5 μm (b, inset).
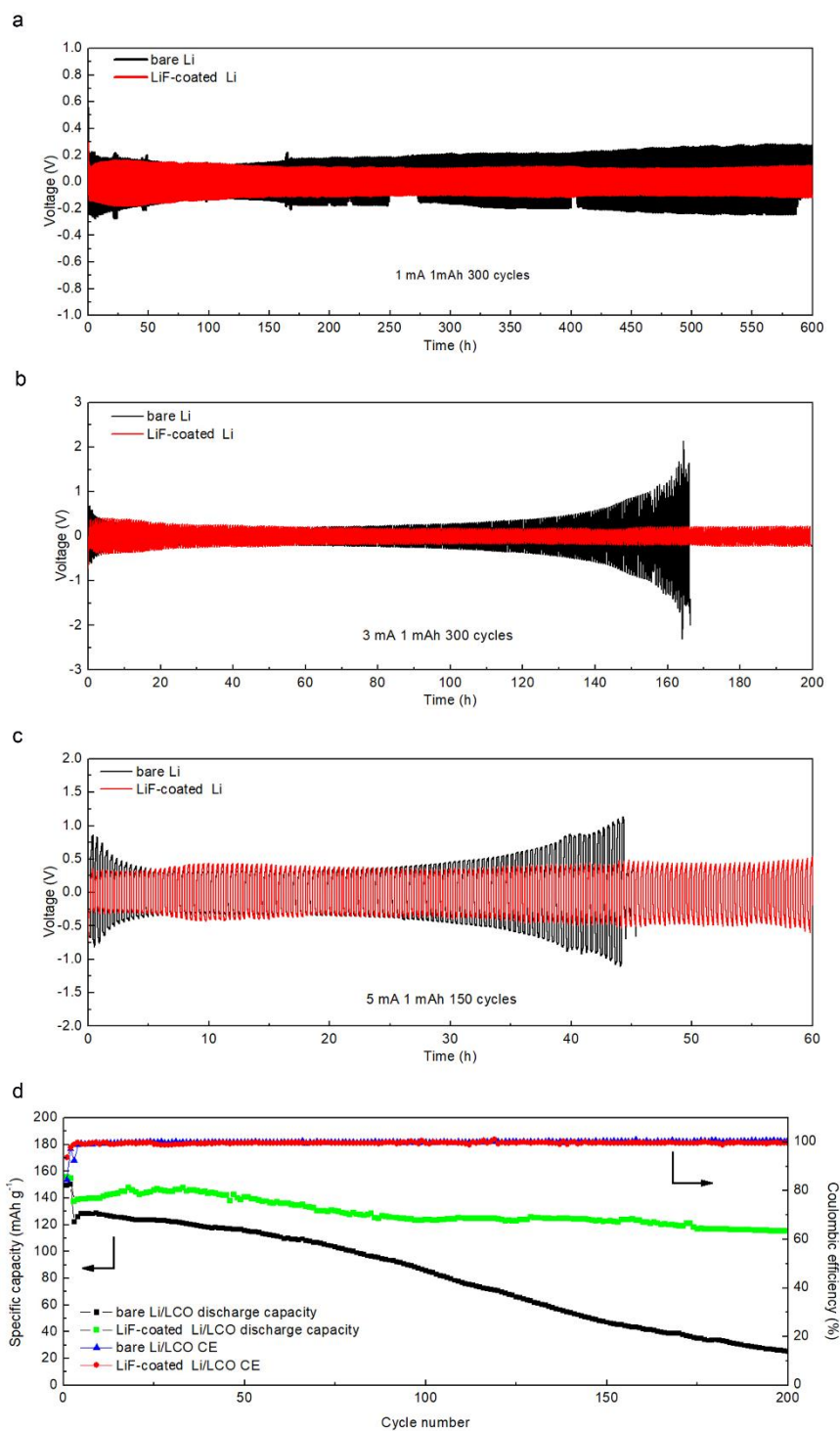
Fig. 4. Electrochemical characterization of LiF-coated Li metal. A comparison of the cycling stability of the symmetric LiF-coated Li metal (red) and bare Li metal (black) cells with carbonate electrolytes at a current density of (a) 1 mA cm^{-2}, (b) 3 mA cm^{-2}, and (c) 5 mA cm^{-2}, respectively. (d) The cycling performance of the LiF-coated Li|LiCoO$_2$ cell. The first two cycles were at the current density of 0.2 mA cm^{-2}, and then the current density was raised to 1 mA cm^{-2}.
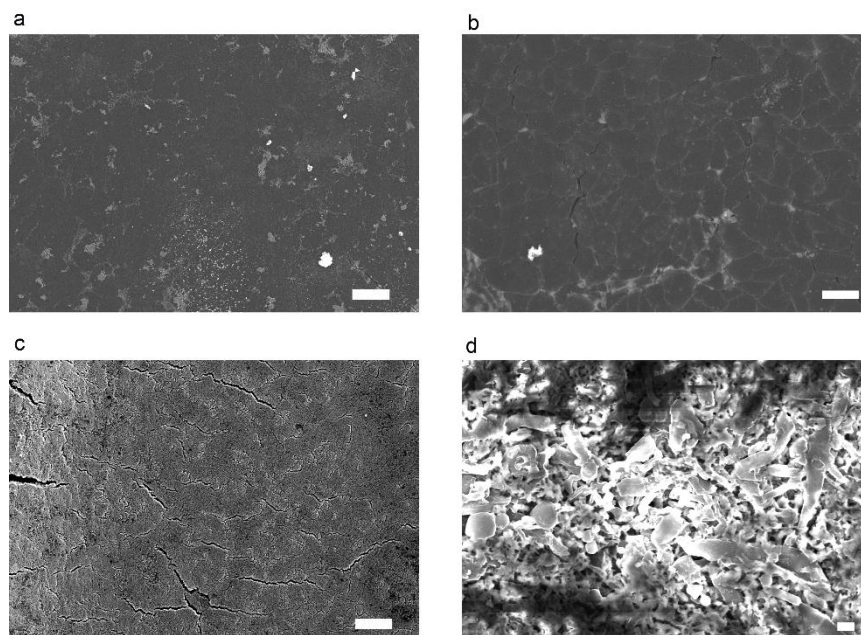
Fig. 5. SEM images of (a, b) LiF-coated Li electrode and (c, d) bare Li electrode after 100 cycles at a current density of 1 mA cm^{-2}. Scale bar, 100 μm (a, c), 10 μm (b) and 1 μm (d).